The Eurasia Proceedings of Science, Technology, Engineering & Mathematics (EPSTEM)
ISSN: 2602-3199

The Eurasia Proceedings of Science, Technology, Engineering & Mathematics (EPSTEM), 2022

Volume 21, Pages 88-95

IConTES 2022: International Conference on Technology, Engineering and Science

Fluid-Structure Interaction: Impact of Reservoir Simulation Approach Considering Far-Field Boundary Condition in Dam Seismic Response

Reza GOLDARAN
Cyprus International University (CIU)

Abstract: Given the vitality of dams to life and the catastrophe caused by their failure, an adequate safety margin must be considered while designing for permanent and transient loads. Neglecting the transient loads in design make the dam structure vulnerable to damage; consequently, the earthquake load is crucial as a transient dynamic load. The horizontal component of an earthquake causes acoustic waves to exert hydrodynamic pressure on the dam's upstream face in addition to hydrostatic pressure. This study aims to assess the dynamic response of a dam using Lagrangian-Lagrangian and Lagrangian-Eulerian modeling approaches for a solid-liquid interaction. To this end, as a case study, time-domain analysis is carried out using ANSYS to determine the PINE FLAT dam response subjected to the horizontal component of the TAFT ground motion. The results indicate that considering the following points, the dam's dynamic responses in both approaches are almost identical. In order to absorb the scattered acoustic waves in the Eulerian reservoir, a condition involving a particular boundary element at the far field with a specific geometry must be provided. Also, the length-to-height ratio of the reservoir must not be less than a specific value in the Lagrangian fluid to minimize the effect of propagated acoustic wave reverberation.

Keywords: Fluid-structure interaction, Hydrodynamic pressure, Concrete dam, Added mass, Dam reservoir interaction

Introduction

Dams are essential for the supply of water resources, yet their failure may inflict severe consequences on a country's economy. Therefore, it seems necessary to investigate the behavior of dams in different conditions. The dynamic dam–reservoir interaction upon an earthquake has been demonstrated to be a crucial parameter in the design of such structures. Failure to incorporate the dynamic load of earthquakes into the design of a dam would lead to seismic damage to the structure. Furthermore, the overdesign of the dam would lead to an uneconomic structure.

Westergaard (Westergaard, 1933) modeled hydrodynamic pressure on a gravity dam two-dimensionally under horizontal ground motions, assuming a rigid dam body with a vertical upstream surface, horizontal bottom, and the reservoir as a continuum of infinite length. It was found that a portion of the reservoir would vibrate with the dam body, and the hydrodynamic force is distributed parabolically along the dam height, referred to as Westergaard's added mass (Feltrin, 1997). Zengar (Zangar & Haefeli, 1952) pursued Westergaard's work and demonstrated that his theory's validity was satisfactory. Chopra (Chopra & Chakrabarti, 1973) investigated the effects of water compressibility and dam flexibility on the dam-reservoir interaction. They showed that the stable response of pressure would not be damped by moving away from the reservoir when the loading frequency is higher than the first mode frequency of the reservoir, and it would be propagated. The Department of Earthquake Engineering (Council, 1991) invalidated Westergaard's added mass due to significant errors. With the development of numerical methods in the 1970s, Fin (Finn & Varoğlu, 1973) adopted the finite element method (FEM) to solve the dam–reservoir interaction equations. Some studies investigated boundary conditions

- Selection and peer-review under responsibility of the Organizing Committee of the Conference

in the dam–reservoir interaction, among which the major one is applying Sommerfeld's boundary condition for the far end of the infinite reservoir (Kucukarslan, 2005).

The influence of reservoir length on the seismic response of gravity dams subjected to ground motions from local and far faults was investigated by Bayraktar (Bayraktar et al., 2010). Using Lagrangian (Akkose & Simsek, 2010) and Eulerian (Altunisik et al., 2019) approach, an investigation was carried out to determine the nonlinear seismic performance of concrete gravity dams exposed to near and far fault motions. Sevim (Sevim et al., 2011) demonstrated the impacts of water height and length on the seismic reactivity of arch dam-reservoir-foundation configurations considering the Lagrangian viewpoint.

The nonlinear seismic assessments of concrete gravity dams performed by Wang (Wang et al., 2012) involved utilizing a 3D dam model that accounted for the hydrodynamic influences of the impounded water. The absorbing boundary conditions for vibration analysis were investigated by Samii (Samii & Lotfi, 2013). The research was conducted by Wick (Wick, 2013) regarding the coupling of arbitrary Lagrangian-Eulerian approaches and fully Eulerian for the purpose of fluid-structure interaction (FSI) simulations. In addition to dams, FSI would be of the utmost importance in pipelines, where it may, in conjunction with corrosion, lead to pipe bursting and have disastrous effects. It is possible to identify damages at an early stage by utilizing various damage detection strategies, such as those based on vibration and ultrasonic waves. (Goldaran & Kouhdaragh, 2021; Goldaran & Turer, 2020). Scholars have implemented a variety of investigations in order to evaluate the seismic responses of dams by taking into account the interactions between the various components of dam-reservoir-sediment-foundation systems (Baghban et al., 2021; Girme & Waghmare, 2021; Mandal & Maity, 2018; Moallemi et al., 2020; Srivastava & Sahoo, 2022; Yazdani & Alembagheri, 2017).

In the current work, the dynamic response of a dam was assessed using Lagrangian-Lagrangian and Lagrangian-Eulerian methods for a solid-liquid interaction. To evaluate the effect of the horizontal component of the TAFT earthquake on the PINE FLAT dam - as a case study - a time-domain analysis is performed with ANSYS. In both approaches, the dam's dynamic responses are almost equivalent. A far-field boundary element must be involved to absorb scattered acoustic waves in the Eulerian reservoir. For mitigating wave reverberation, the reservoir's length-to-height ratio must not be less than a specific value in the Lagrangian fluid.

Dam–reservoir system equations

The dam–reservoir interaction is obtained by solving two coupled quadratic differential equations. The differential equations of the structure and reservoir are written as follows:

$$[M]\{\ddot{u}\} + [C]\{\dot{u}\} + [K]\{u\} = \{f_1\} - [M]\{\ddot{u}_{gh}\} - [M]\{\ddot{u}_{gv}\} + [Q]\{P_h(t)\} \quad (1$$

$$[G]\{P_h\} + [C']\{\dot{P}_h\}[K']\{P_h\} = \{f_2\} - \rho[Q]^T\{\ddot{u}\} \quad (2$$

Where [M], [C], and [K] are the mass, damping, and stiffness matrices of the dam, while [G], [C'], and [K'] are the mass, damping, and stiffness matrices of the reservoir, respectively. Furthermore, [Q] is the coupled structure–reservoir matrix, $\{f_1\}$ denotes the vector of body and hydrostatic forces, $\{f_2\}$ represents the vector of the acceleration-induced forces on the dam–reservoir interface, {P} is the pressure vector, {u} is the displacement vector, $\{\ddot{u}_g\}$ is the gravitational acceleration vector, and ρ is the fluid density. According to Fig. 1, with the assumption of compressible, non-viscous, and irrotational fluid, the governing equations of the reservoir domain for flexible dam bodies considering the given boundary conditions are in the form of relations (3) to (7).

$$\nabla^2 P = \frac{1}{C^2}\frac{\partial^2 P}{\partial t^2} \quad \text{boundary condition } \Omega_f \quad (3$$

$$\frac{\partial P}{\partial n} = -\rho a_g^n \quad \text{boundary condition } \Gamma_1 \quad (4$$

$$\frac{\partial P}{\partial n} = 0 \quad \text{boundary condition } \Gamma_2 \quad (5$$

$$P = 0 \quad \text{boundary condition } \Gamma_3 \quad (6$$

$$\frac{\partial P}{\partial n} = -\frac{1}{C}\frac{\partial P}{\partial t} \quad \text{boundary condition } \Gamma_4 \quad (7$$

Sommerfeld's boundary condition may be employed at the end of the reservoir to absorb acoustic waves. Sommerfeld's boundary condition (Eq. (7)) is an approximate solution in which P, *t*, and *n* are pressure, time, and normal vector, respectively.

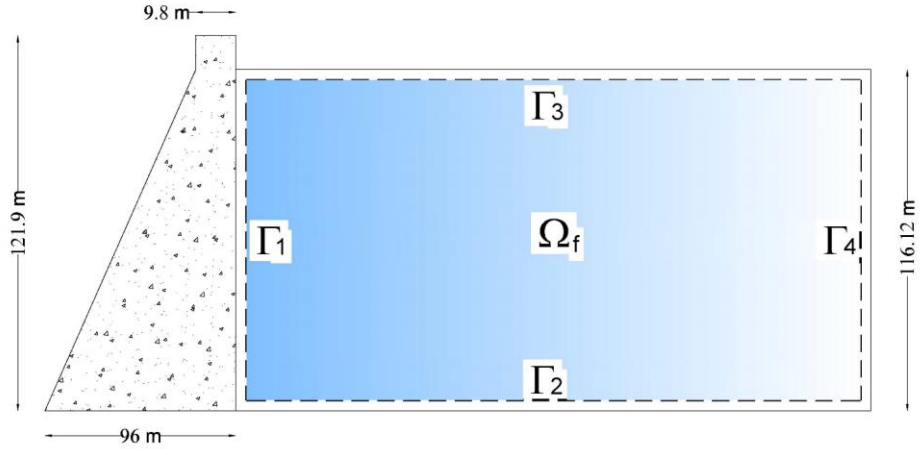

Figure 1. Pine flat dam geometry along with boundary condition

Its approximate solution is because of the ability to absorb only one-dimensional, normal waves. The Impedance boundary condition was employed to provide acoustic wave absorption at the far end of the reservoir. In applying this wave absorption condition, the reservoir is modeled in a rectangle fashion, and likely satisfies the Summerfield boundary condition. Water's dynamic viscosity (MU) must be set to 1 to meet the mentioned boundary condition.

Method

For simulating the dam-reservoir interaction and analyzing the model, ANSYS software was utilized. As mentioned earlier, the present work investigated the PINE FLAT dam under the horizontal ground motion records of the TAFT earthquake. Figure 1 and Tables 1 to 3 represent the specification of geometry and material properties of both the dam body and reservoir.

Table 1. Geometry of dam body

Height (m)	Crest width (m)	Bottom width (m)	Upstream slope	Downstream slope	Water level (m)
121.90	9.80	96	1 to 0.05	1 to 0.78	116.12

Table 2. Reservoir specification

Water Density (kg/m^3)	Acoustic wave velocity in water (m/s)	Reservoir bottom absorption factor	Viscosity (Mpa.s)	Bulk modulus (kg/cm^2)	Poison ratio	length (m)
1000	1440	0.5	1.307	2.1e8	0.49	300

Table 3. Material (concrete) properties of dam body

Density (kg/m^3)	E (kg/cm^2)	Poison ratio	Damping ratio (%)
2500	2.785e9	0.2	5

Euler–Lagrange model

The Plane182 element was exploited for the dam body. Plane182 is a four-node element with two translational degrees of freedom (U_x, U_y) in each node. The Fluid29 element was employed to model the reservoir. It is a four-node element with two translational and one pressure degree of freedom (U_x, U_y, and P) in each node. It has the ability to model acoustic waves and includes the wave absorption factor. The dam structure was modeled under two settings:

(I) keypoint(2) = 0 for elements in contact with the solid surface (dam structure)
(II) keypoint(2) = 1 for elements not in contact with the solid surface, as shown in Figure 2.

The FLUID129 acoustic wave absorption element was employed at the end of the reservoir to model the far end (semi-infinite) and satisfy Sommerfeld's boundary condition. A FLUID129 is a 2-node element and must lie on a circular boundary and entirely contain the domain meshed with FLUID29 elements, as shown in Fig. 2. For the best results, the circle's center should be placed as close to the model's center as possible.

In the present work, MU was set to 0.5 in the Fluid29 element to define the bottom absorption conditions. It varies from 0 (no absorption) to 1 (full absorption) and may even be higher than 1 in some cases.

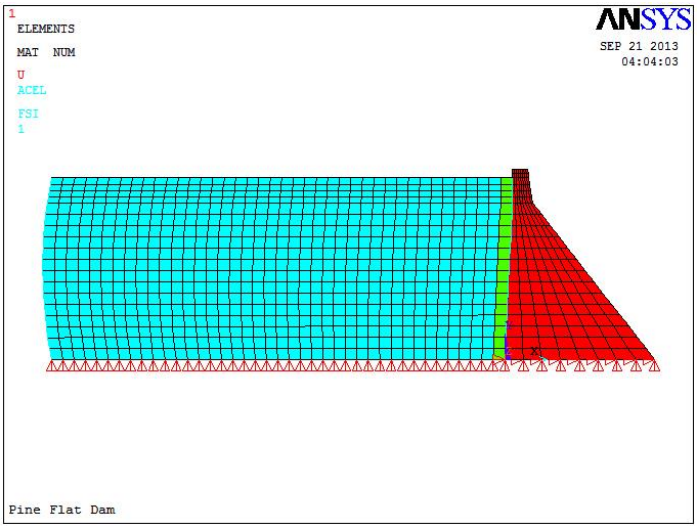

Figure 2. Eulerian-Lagrangian simulation

Dynamic Analysis of the Dam under Horizontal Ground Motions

The ANSYS Parametric Design Language (APDL) is utilized to import the ground motion time-history record. The 14-second horizontal component of the TAFT earthquake record was introduced at a 0.02-second increment in TRANSIENT analysis. Figure 3 represents the ground-motion accelerogram of the TAFT earthquake prepared by SeismoSignal.

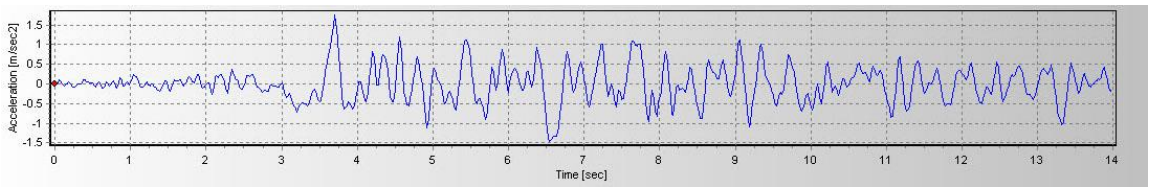

Figure 3. Ground-motion accelerogram of Taft earthquake

Coupling

Since the model consisted of both fluid and solid phases; hence, coupled field analysis was employed. To this end, it was required to couple the reservoir and dam on the interface, which could be carried out using either sequential or direct analysis.

Sequential analysis

In this procedure, numerous consecutive analyses are undertaken, each pertaining to a different field.

Direct analysis

To conduct an FSI analysis with this method, coupling participants are linked to a component system named System Coupling. A system that contributes to or receives data in a coupled analysis is called a participant

system. Here, there are two coupling participants: Fluent (the first) and ANSYS Mechanical (the second). System coupling first gathers data from the participants to synchronize the simulation's whole setup, and the information that needs to be shared is then given to the respective participant. The following phase is to organize the sequence of the exchange of information. Ultimately, at the end of each coupling iteration, the convergence of the coupling step is evaluated.

It is noteworthy that direct analysis requires coupled-field elements. The present work adopted direct analysis considering Fluid29 is a coupled-field element. Figure 4 shows the deformed shape of the dam body under direct analysis, and Fig. 5 and table 4 represent the time history and maximum displacement of the dam crest, respectively. Figure 6 plots the analysis result of the model excluding the Fluid129 element. As shown, ignoring the Fluid129 absorption element disturbed the responses.

Lagrange–Lagrange model

The Solid65 element was employed to model the dam body. In this 8-node element, each node has three transitional degrees of freedom (U_x, U_y, U_z). The reservoir was modeled with the 8-node Solid185 element in which each node has three transitional degrees of freedom (U_x, U_y, U_z). This element has the capability of large deflection without entering the nonlinear phase. The dam-reservoir interface was modeled using the Contact178 element with axial and shear stiffness of 10e10 kg/cm^2. This element's parameters are set so that it transmits compressive force but does not resist tensile loads. A friction coefficient (MU) of 0.2 was set for the Contact178 element.

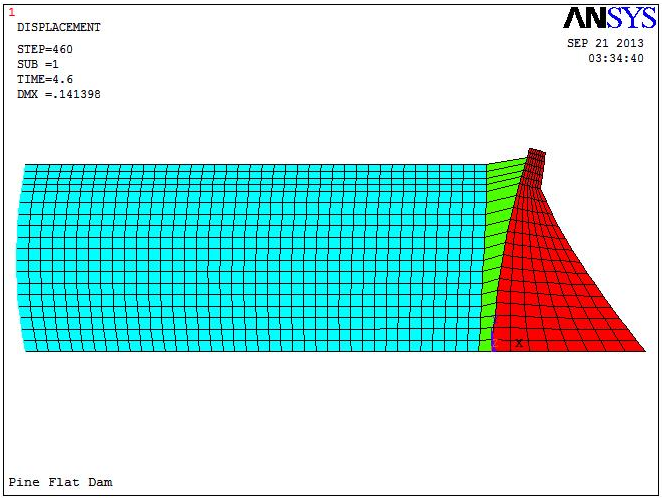

Figure 4. Deformed shape of dam body

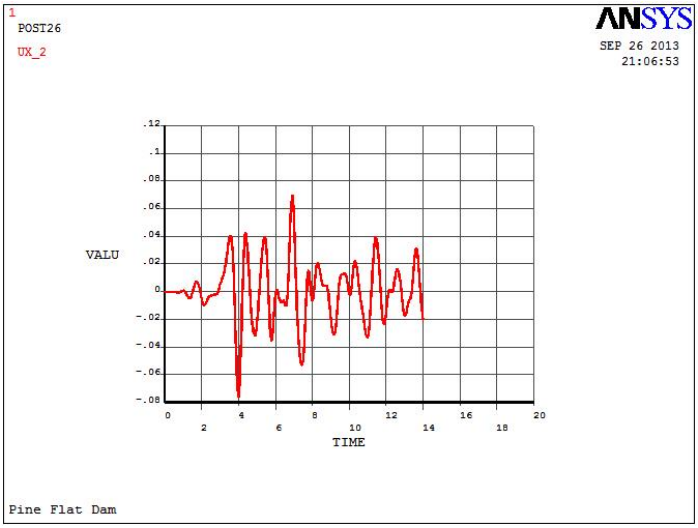

Figure 5. Displacement time history at the dam crest level

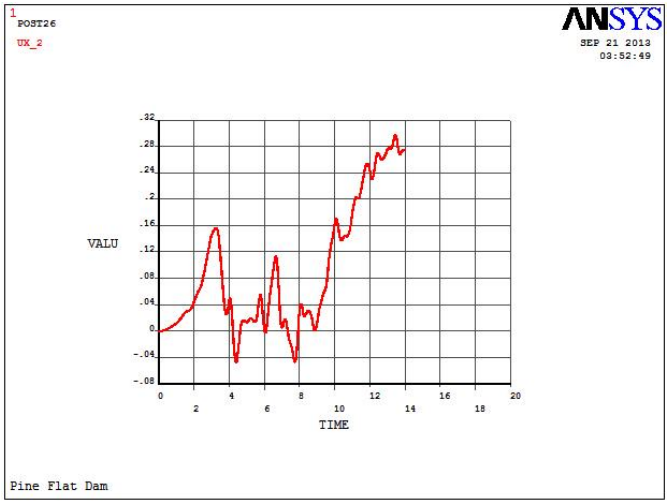

Figure 6. Displacement time history at the dam crest level in the absence of acoustic wave absorption element

The critical point is the correct application of the restrictions of the support. All dam body's nodes in contact with the ground were constrained in all directions, and the reservoir nodes in contact with the ground or semi-infinite boundary were constrained only in one direction so that, in practice, it is not also possible for the fluid to move in that direction. Figure 7a illustrates the dam model, and Fig. 7b represents the displacement time history of the dam crest applying the Lagrange–Lagrange approach. Table 4 reports the maximum displacement of the dam crest induced by both procedures. It may be seen that considering the following conditions, both methods lead to approximately the same response. In the Lagrangian-Lagrangian simulation, the length-to-height ratio of the reservoir must be large enough to mitigate the wave reflection (here, it was limited to 2.5).

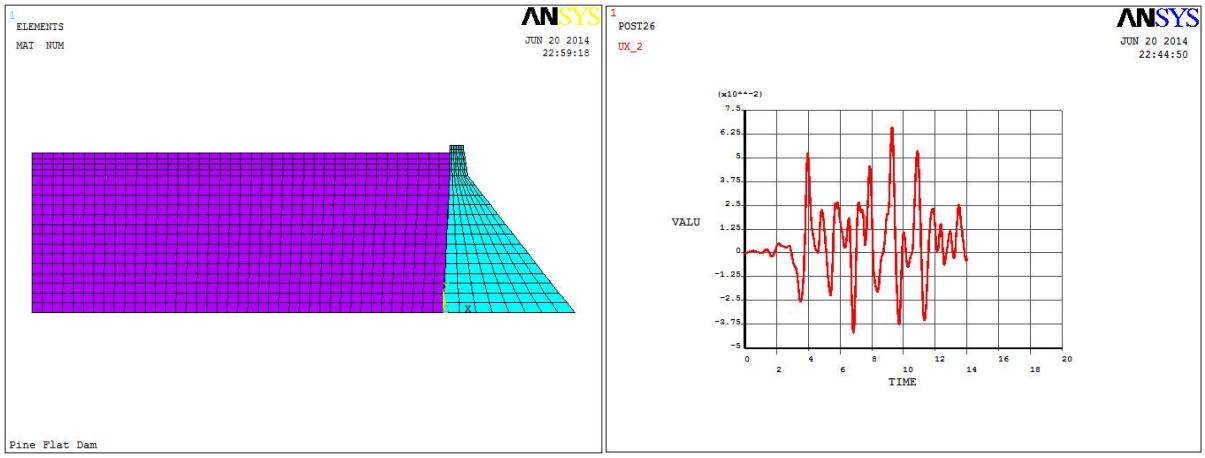

Figure 7. a) Lagrangian – Lagrangian simulation, b) Displacement time history at the dam crest level

Table 4. Maximum displacement of the dam crest

Lagrange–Lagrange method (m)	Euler–Lagrange method (m)
0.068	0.065

Conclusion

In the present work, the dynamic response of the PINE FLAT dam, as a case study, due to FSI under the TAFT earthquake was carried out using ANSYS to illustrate the results derived from two different perspectives, the Lagrangian-Lagrangian, and Lagrangian-Eulerian approaches. It is concluded that both methods are very effective, efficient, and capable of producing almost identical results (error < 5%) to any desired degree of accuracy considering the following points.

- A condition including a particular boundary element at the far field with a specific geometry is required to absorb the scattered acoustic waves in the Eulerian reservoir. To achieve this goal, the FLUID129

acoustic wave absorption element was used, which is a 2-node element and must lie on a circular boundary and totally encapsulate the domain meshed with FLUID29 elements.

- For the best results, the generated circle's center by the mentioned 2-node boundary element should be as close to the model's center as possible.
- In the Lagrangian-Lagrangian simulation, the length-to-height ratio of the reservoir, which is restricted to 2.5 in the present study, must be large enough to minimize the effect of propagated acoustic wave reflection.
- Excluding wave absorption elements at the Eulerian reservoir's far end led to unreliable results.

Scientific Ethics Declaration

The author declares that the scientific ethical and legal responsibility of this article published in EPSTEM journal belongs to author.

Acknowledgements or Notes

* This article was presented as an oral presentation at the International Conference on Technology, Engineering and Science (www.icontes.net) conference held in Antalya/Turkey on November 16-19, 2022.

References

Akkose, M., & Simsek, E. (2010). Nonlinear seismic response of concrete gravity dams to near-fault ground motions including dam-water-sediment-foundation interaction. *Applied Mathematical Modelling*, *34*(11), 3685–3700.

Altunisik, A. C., Sesli, H., Husem, M., & Akkose, M. (2019). Performance evaluation of gravity dams subjected to near-and far-fault ground motion using Euler approaches. *Iranian Journal of Science and Technology, Transactions of Civil Engineering*, *43*(2), 297–325.

Baghban, M. H., Faridmehr, I., Goldaran, R., & Amoly, R. S. (2021). Seismic analysis of concrete arch dam considering material failure criterion. *IOP Conference Series: Materials Science and Engineering*, *1117*(1), 12004.

Bayraktar, A., Turker, T., Akkose, M., & Ates, S. (2010). The effect of reservoir length on seismic performance of gravity dams to near-and far-fault ground motions. *Natural Hazards*, *52*(2), 257–275.

Chopra, A. K., & Chakrabarti, P. (1973). Dynamics of gravity dams-significance of compressibility of water and three dimensional effects. *International Journal of Earthquake Engineering and Structural Dynamics*, *2*, 103–104.

Council, N. R. (1991). *Earthquake engineering for concrete dams: design, performance, and research needs*. National Academies Press.

Feltrin, G. (1997). *Absorbing boundaries for the time-domain analysis of dam-reservoir-foundation systems* (Vol. 232). ETH Zurich.

Finn, W. D. L., & Varoğlu, E. (1973). Dynamics of gravity dam-reservoir systems. *Computers & Structures*, *3*(4), 913–924.

Girme, P. D., & Waghmare, M. V. (2021). Effect of dam reservoir interaction on response of dam subjected to dynamic load. In *Recent Trends in Civil Engineering* (pp. 945–961). Springer.

Goldaran, R., & Kouhdaragh, M. (2021). Structural health monitoring of beams with moving oscillator: theory and laboratory. *Građevinar*, *73*(07.), 693–704.

Goldaran, R., & Turer, A. (2020). Application of acoustic emission for damage classification and assessment of corrosion in pre-stressed concrete pipes. *Measurement*, *160*, 107855.

Kucukarslan, S. (2005). An exact truncation boundary condition for incompressible–unbounded infinite fluid domains. *Applied Mathematics and Computation*, *163*(1), 61–69.

Mandal, K. K., & Maity, D. (2018). Transient response of concrete gravity dam considering dam-reservoir-foundation interaction. *Journal of Earthquake Engineering*, *22*(2), 211–233.

Moallemi, R., Mahboubi, B., Bakhtiari, P., Rezaiy, R., & Manalo, O. (2020). Seismic performance of concrete reservoirs considering soil-structure-fluid interaction under near-and far-field seismic excitations. *Journal of Civil Engineering and Materials Application*, *4*(1), 55–73.

Samii, A., & Lotfi, V. (2013). A high-order based boundary condition for dynamic analysis of infinite reservoirs. *Computers & Structures*, *120*, 65–76.

Sevim, B., Altunssik, A. C., Bayraktar, A., Akkose, M., & Calayir, Y. (2011). Water length and height effects on the earthquake behavior of arch dam-reservoir-foundation systems. *KSCE Journal of Civil Engineering*, *15*(2), 295–303.

Srivastava, R. K., & Sahoo, D. R. (2022). Seismic analysis of a concrete gravity dam considering dam-water-sediment-foundation interaction. *Dams and Reservoirs*, 1–27.

Wang, H., Feng, M., & Yang, H. (2012). Seismic nonlinear analyses of a concrete gravity dam with 3D full dam model. *Bulletin of Earthquake Engineering*, *10*(6), 1959–1977.

Westergaard, H. M. (1933). Water pressures on dams during earthquakes. *Transactions of the American Society of Civil Engineers*, *98*(2), 418–433.

Wick, T. (2013). Coupling of fully Eulerian and arbitrary Lagrangian–Eulerian methods for fluid-structure interaction computations. *Computational Mechanics*, *52*(5), 1113–1124.

Yazdani, Y., & Alembagheri, M. (2017). Nonlinear seismic response of a gravity dam under near-fault ground motions and equivalent pulses. *Soil Dynamics and Earthquake Engineering*, *92*, 621–632.

Zangar, C. N., & Haefeli, R. J. (1952). Electric analog indicates effect of horizontal earthquake shock on dams. *Civil Engineering*, *22*(4), 54–55.

Author Information

Reza Goldaran
Cyprus International University (CIU)
Nicosia, Northern Cyprus
Contact e-mail: *rezagoldaran@gmail.com*

To cite this article:

Goldaran, R. (2022). Fluid-structure interaction: Impact of reservoir simulation approach considering far-field boundary condition in dam seismic response. *The Eurasia Proceedings of Science, Technology, Engineering & Mathematics (EPSTEM), 21*, 88-95.